APPENDIX B

Analysis of Photographic Grain Size Beach Surface Sediment in Rich Passage

Grain Size Analysis of Beach Sediment in Rich Passage Washington, August 3, 2004. A Report prepared for Pacific International Engineering

Thanos Papanicolaou* and Kyle Strom†

The objective of the authors was to determine grain size distributions of the surface material in the 28 images provided by Pacific International Engineering. The 28 images were collected on August 3, 2004 by Pacific International Engineering at beach monitoring sites 1, 3, 4, 5, 7, 9 and 10 located in Rich Passage Washington as part of the Rich Passage Wake Impact Study. At the time of sampling Rights-of-Entry had not been obtained for properties on which Sites 2, 6, 11, 12, and 13 are located (personal communication, Phil Osborne, PI Engineering 10/21/2004).

1 Automated Grain Size Analysis

There are three basic steps in determining grain size distributions from digital images.

1. Identification of particles
2. Measurement of particle dimensions
3. Numerical sieving

Image analysis techniques have been shown to work well in identifying and measuring particles in well lit images (Butler et al., 2001; McEwan et al., 2000), and hence are powerful tools for computing grain size distributions of large amounts of particles.

*Associate Professor, Dept. Civil and Envir. Engr., IIHR–Hydroscience & Engineering, University of Iowa, Iowa City, IA 52242, USA, e-mail: apapanic@engineering.uiowa.edu, phone: 319 335 6448,

†Graduate Research Assistant; Dept. Civil and Envir. Engr., IIHR–Hydroscience & Engineering, University of Iowa, Iowa City, IA 52242-1585, e-mail: strom@engineering.uiowa.edu,

Inherent in all image analysis particle size extraction is the assumption that the small visible particle axis of a particle is the true b axis as would be measured if the particle were picked up, where the b axis refers the intermediate axis of a particle (Adams, 1979; Butler et al., 2001; McEwan et al., 2000). This assumption has been shown to be a fairly good assumption (Adams, 1979; McEwan et al., 2000; Butler et al., 2001), but does not universally hold true due to such things as particle orientation, hiding, imbrication, embeddedness, and particle size relative to the field-of-view of the image. Added complications can arise in the case that the image is not taken parallel to the bed. Attempts to correct for these assumptions have not been considered in the present study. While the grain sizes derived from the images might not exactly match grain sizes determined from physically picking up and measuring the particles, the automated grain size analysis does properly measure the sized of the particles in the image (Butler et al., 2001).

2 Methodology

Grain size distributions of the surface material in the images were computed with the use of the image analysis software ImageJ 1.32j (`http://rsb.info.nih.gov/ij/`) and IGOR Pro 5.03 (`http://www.wavemetrics.com/`). This section outlines the basic procedures followed to obtain a size distribution for each image.

For the first step of this process, each image is opened and the pixel to physical length scale is set and recorded. The image is then cropped to remove the scale, and converted to an 8-bit greyscale Fig. 1. The image threshold is then set to produce a binary image where black represents the particles and white the voids. A watershed function is then applied to separate particles that might be touching, resulting in Fig. 2. At this point the image has been properly conditioned for automated grain size analysis, and equivalent ellipses are fit to each particle in the watershed image Fig. 3. The assumption is then made that the minor axis of the ellipse is the b-axis as it would be measured in the field.

An in house automated procedure for IGOR Pro was developed to handle b-axis output from Image J as input and return a corresponding areal, frequency-by-number grain size distribution (Kellerhals and Bray, 1971) in 0.5ϕ increments, where ϕ is defined as,

$$\phi = -\log_2 d \tag{1}$$

Figure 1: Image P8030129 at Site 1 after it has been cropped and greyscaled

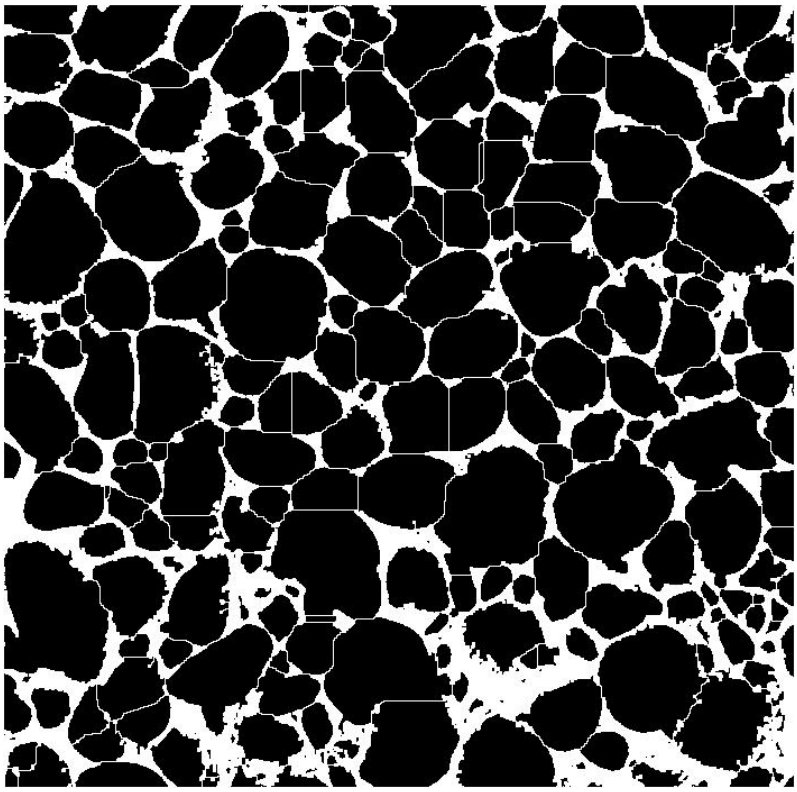

Figure 2: Image P8030129 at site one after thresholding and watersheded.

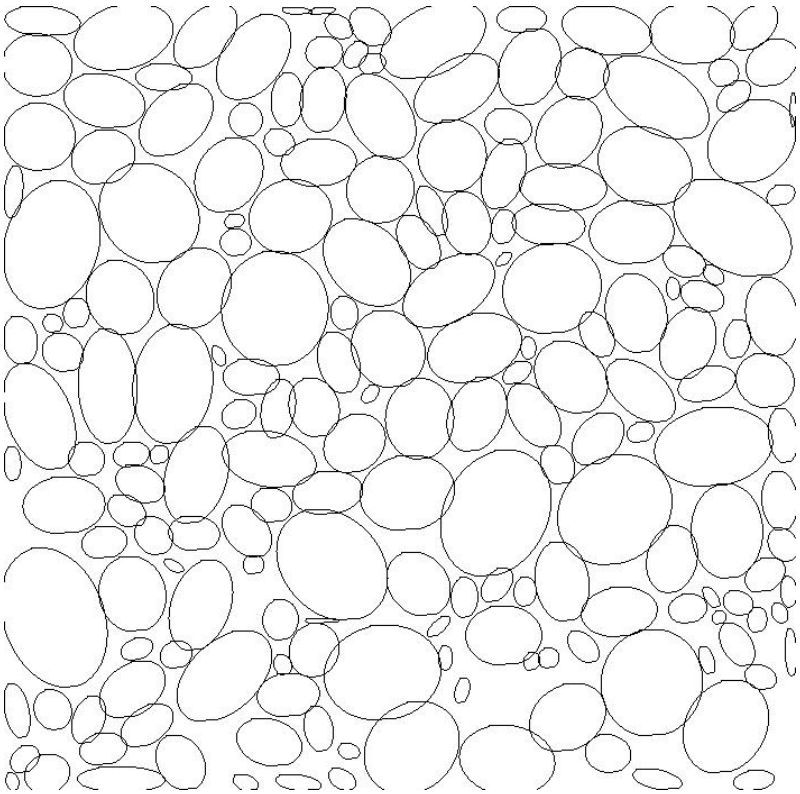

Figure 3: Fit ellipse for Image P8030129

and d is particle diameter in mm. The following formula can be used to convert ϕ units and mm: $\phi_i = -3.3219 \log_{10} d_i$ and $d_i = 2^{-\phi_i}$.

In order to make conclusions about bed composition, an areal, frequency-by-number grain size distribution must be converted to an equivalent volumetric, frequency-by-weight distribution. To do this, the number of particles in each size class is weighted by d_i^2 (Kellerhals and Bray, 1971) as follows, $(P_{nA})_i = (P_n)_i d_i^2$; where $(P_{nA})_i$ is the adjusted number of particles in size fraction i, $(P_n)_i$ is the original number of particle in size fraction i, and d_i is the particle diameter in size class i. This accounts for the greater percentage of area that particles of larger diameter occupy compared to particles of lesser diameter. Fig. 4 displays the weighted and unweighted distribution for image P8030129.

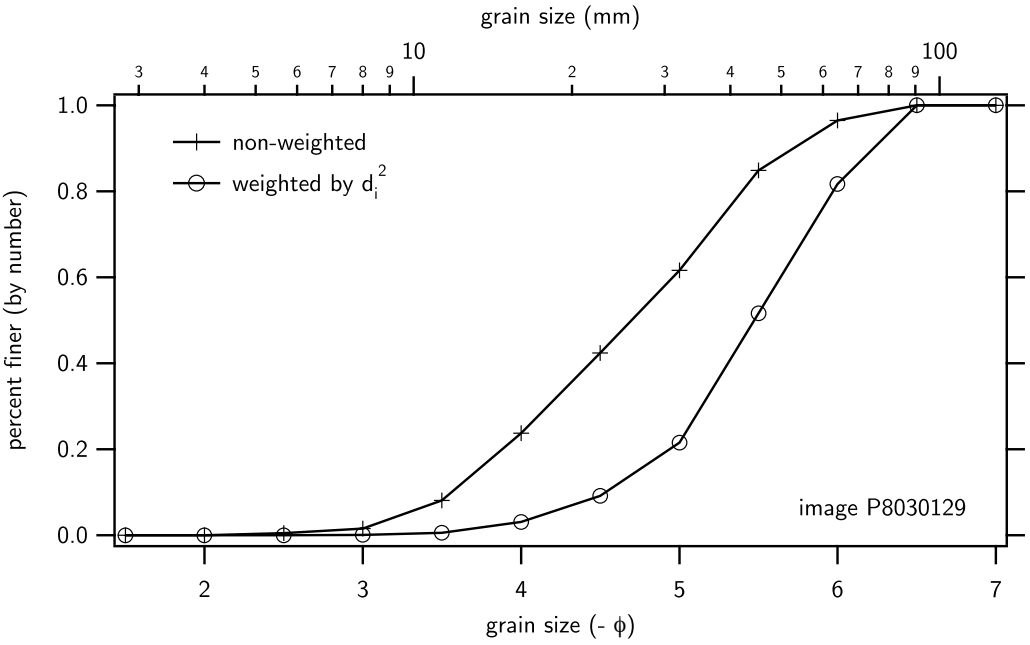

Figure 4: Weighted and unweighed grain size distribution for image P8030129

2.1 Error

No direct quantification of the error associated with the grain size distribution resulting from the image compared to a distribution from a grid, frequency-by-number or sieved, frequency-by-weight analysis could be made. Error between the two methods is site specific (e.g. Adams, 1979; Church et al., 1987) and requires direct sampling of the imaged surface material. It can be expected that a distribution measured

from an image would underestimate particle size by some factor due to conditions such as imbrication, particle packing, and embeddedness. Adams (1979) and Butler et al. (2001) note that use of the b-axis in particle sizing techniques from images does produce a systematic bias where the distribution found from the image underestimates the true distribution by some factor. It is the authors' experience from automated grain size extraction on gravel river bars, that grain size information extracted from images and weighted with a d_i^2 weighting is fairly robust. The automated grain size extraction technique typically produces differences in d_{16}, d_{50}, and d_{84} from that determined by pebble counts, following Wolman (1954), that fall with the 95% percentile precision confidence limits of Rice and Church (1996) for their associated percentiles.

3 Results

Tables 1 & 2 presents a summary of the analysis in ϕ units and mm respectfully. Grain size distribution plots are organized by site and are presented in Fig. 5–34.

Images P8030031, P8030073, and P8030085 were not well suited for automated grain size analysis. For these images it was not possible to identify individual grains, as the image analysis program tended to clump particles together due to the size of the particles compared to the resolution and the lighting.

Difficulty in obtaining accurate particle identification in image P8030099 was also encountered and summary statistics from this image should be check by manual pebble counts if high accuracy of the grain size statistics is required.

Also, automated grain sizes information could not be obtained from image P8030112 due to the large range of particle sizes and particle colors present in the image. In P8030112, the image was overlaid with a grid and particles falling underneath grid intersection points where measured. This technique does not require any weighting as the greater area occupied by the larger particles is already accounted for (Kellerhals and Bray, 1971). However, for this image, the grain size distribution is likely to be biased towards the larger particles as the resolution of the image impeded the identification of the smaller particles.

Some images that displayed patches of different size distributions in the same image were broken down into sub-image sets. Image P8030007 is an example of this. This image was broken down into "larger" particles in the top of the image, "smaller" particles at the bottom, and all particles combined in the top of the image (Table Tables 1 & 2).

site	image	d_{16} $(-\phi)$	d_{50} $(-\phi)$	d_{84} $(-\phi)$	σ_g $(-\phi)$	d_{min} $(-\phi)$	d_{max} $(-\phi)$	# particles
1	P8030125	3.99	4.48	4.97	1.40	2.79	5.59	438
1	P8030129	4.78	5.47	6.06	1.56	2.31	6.13	198
1	P8030131	5.02	5.88	6.31	1.56	2.28	6.37	40
3	$P8030007_{top-combined}$	2.82	3.55	4.24	1.64	1.95	4.76	715
3	$P8030007_{top-large}$	2.77	3.54	4.05	1.56	1.77	4.45	293
3	$P8030007_{bottom-small}$	2.53	3.13	4.16	1.76	1.51	5.17	303
3	$P8030009_{all}$	2.79	3.58	4.39	1.75	1.36	5.47	1322
3	$P8030009_{bottom}$	2.78	3.57	4.35	1.72	1.70	5.48	592
3	P8030013	3.38	4.03	4.54	1.49	1.77	5.16	870
3	P8030017	2.79	3.7	4.69	1.93	1.69	5.54	1286
4	P8030023	3.06	3.59	4.09	1.43	1.63	4.46	677
4	P8030026	3.99	4.73	5.46	1.66	1.48	6.21	429
4	P8030030	4.1	4.76	5.48	1.61	1.55	6.32	422
4	P8030031	2.61	3.26	3.95	1.59	1.87	4.48	120
4	P8030040	4.29	5.01	5.46	1.50	0.74	5.84	318
4	P8030041	3.94	4.48	5.00	1.44	2.24	5.45	459
5	P8030055	4.06	4.71	5.32	1.54	2.54	5.90	320
5	P8030058	4.26	4.86	5.38	1.47	2.11	5.62	252
5	P8030059	2.25	2.79	3.36	1.47	1.70	3.87	209
5	P8030060	3.51	4.00	4.49	1.41	2.46	5.06	603
5	P8030062	4.38	4.89	5.46	1.46	2.64	5.97	238
5	P8030069	4.09	4.65	5.19	1.46	2.27	5.48	314
5	P8030072	4.51	5.07	5.49	1.4	2.63	5.82	201
7	P8030081	4.09	4.75	5.44	1.59	2.88	5.95	308
7	P8030084	4.94	5.43	5.84	1.36	2.66	6.10	148
9	P8030096	2.71	3.26	3.89	1.51	1.79	5.04	1312
9	P8030099	4.03	4.72	5.34	1.57	3.02	5.56	280
9	P8030101	5.72	6.16	6.39	1.26	5.06	6.40	6
10	$P8030112_{smaller}$	2.15	2.64	3.2	1.44	1.20	4.20	395
10	$P8030112_{larger-grid}$	2.99	3.63	4.77	1.84	2.52	6.43	45

Table 1: Grain size statistics summary in ϕ units. $\sigma_g = \sqrt{d_{84}/d_{16}}$ in mm, and the # of particles refers to the number or particles identified and measured in the image.

site	image	d_{16} *(mm)*	d_{50} *(mm)*	d_{84} *(mm)*	σ_g *(mm)*	d_{min} *(mm)*	d_{max} *(mm)*	# particles
1	P8030125	16	22	31	1.40	7	48	438
1	P8030129	27	44	67	1.56	5	70	198
1	P8030131	32	59	79	1.56	5	83	40
3	$P8030007_{top-combined}$	7	12	19	1.64	4	27	715
3	$P8030007_{top-large}$	7	12	17	1.56	3	22	293
3	$P8030007_{bottom-small}$	6	9	18	1.76	3	36	303
3	$P8030009_{all}$	7	12	21	1.75	3	44	1322
3	$P8030009_{bottom}$	7	12	20	1.72	3	45	592
3	P8030013	10	16	23	1.49	3	36	870
3	P8030017	7	13	26	1.93	3	47	1286
4	P8030023	8	12	17	1.43	3	22	677
4	P8030026	16	27	44	1.66	3	74	429
4	P8030030	17	27	45	1.61	3	80	422
4	P8030031	6	10	15	1.59	4	22	120
4	P8030040	20	32	44	1.50	2	57	318
4	P8030041	15	22	32	1.44	5	44	459
5	P8030055	17	26	40	1.54	6	60	320
5	P8030058	19	29	42	1.47	4	49	252
5	P8030059	5	7	10	1.47	3	15	209
5	P8030060	11	16	22	1.41	6	33	603
5	P8030062	21	30	44	1.46	6	63	238
5	P8030069	17	25	37	1.46	5	45	314
5	P8030072	23	34	45	1.40	6	56	201
7	P8030081	17	27	43	1.59	7	62	308
7	P8030084	31	43	57	1.36	6	69	148
9	P8030096	7	10	15	1.51	3	33	1312
9	P8030099	16	26	41	1.57	8	47	280
9	P8030101	53	72	84	1.26	33	84	6
10	$P8030112_{smaller}$	4	6	9	1.44	2	18	395
10	$P8030112_{larger-grid}$	8	12	27	1.84	6	86	45

Table 2: Grain size statistics summary in *mm*. $\sigma_g = \sqrt{d_{84}/d_{16}}$ in *mm*, and the # of particles refers to the number or particles identified and measured in the image.

References

Adams, J. (1979). Gravel size analysis from photographs. *Journal of the Hydraulics Division, Proceedings of the American Society of Civil Engineers*, 105(HY10):1247–1255.

Butler, J. B., Lane, S. N., and Chandler, J. H. (2001). Automated extraction of grain-size data from gravel surfaces using digital image processing. *Journal of Hydraulic Research*, 39(5):519–529.

Church, M. A., McLean, D. G., and Wolcott, J. F. (1987). River bed gravels: sampling and analysis. In C. R. Thorne, J. C. B. and Hey, R. D., editors, *Sediment transport in gravel-bed rivers*, pages 43–88. John Wiley & Sons Ltd.

Kellerhals, R. and Bray, D. I. (1971). Sampling procedures for coarse fluvial sediments. *Journal of the Hydraulics Division, Proceedings of the American Society of Civil Engineers*, 97(HY 8):1165–1180.

McEwan, I. K., Sheen, T. M., Cunningham, G. J., and Allen, A. R. (2000). Estimating the size composition of sediment surfaces through image analysis. *Proceedings of the Institute of Civil Engineering: Water and Maritime Engineering*, 142:189–195.

Rice, S. and Church, M. (1996). Sampling surface fluvial gravels: the precision of size distribution percentile estimates. *Journal of Sedimentary Research*, 66(3):654–665.

Wolman, M. G. (1954). A method of sampling coarse river-bed material. *Transactions American Geophysical Union*, 35(6):951–956.

Appendix: Grain Size Distribution Plots

Site 1

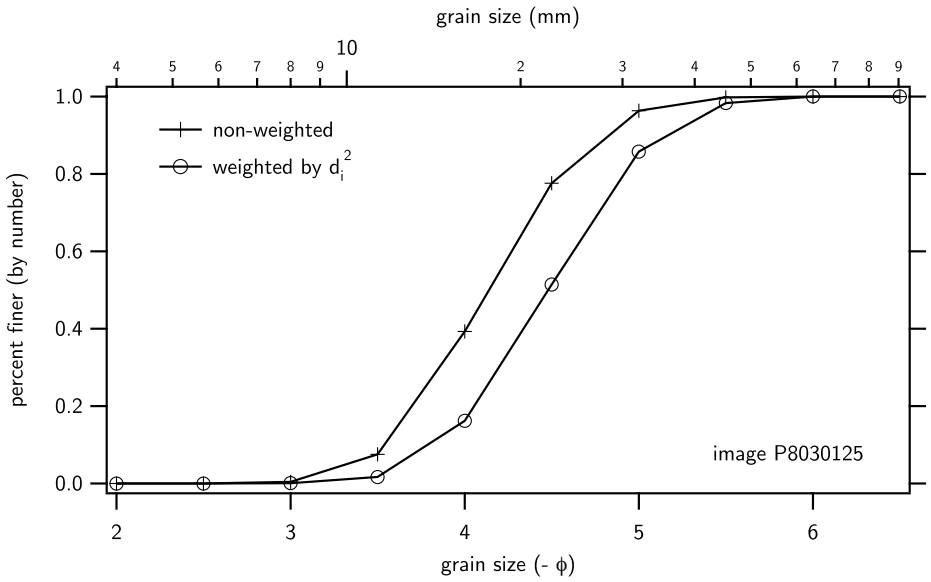

Figure 5: Site 1, image P8030125

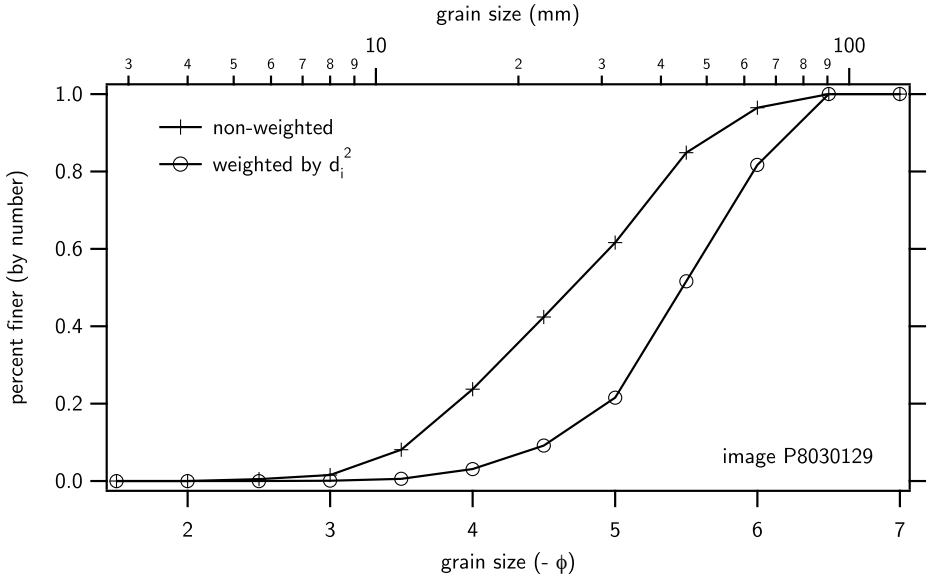

Figure 6: Site 1, image P8030129

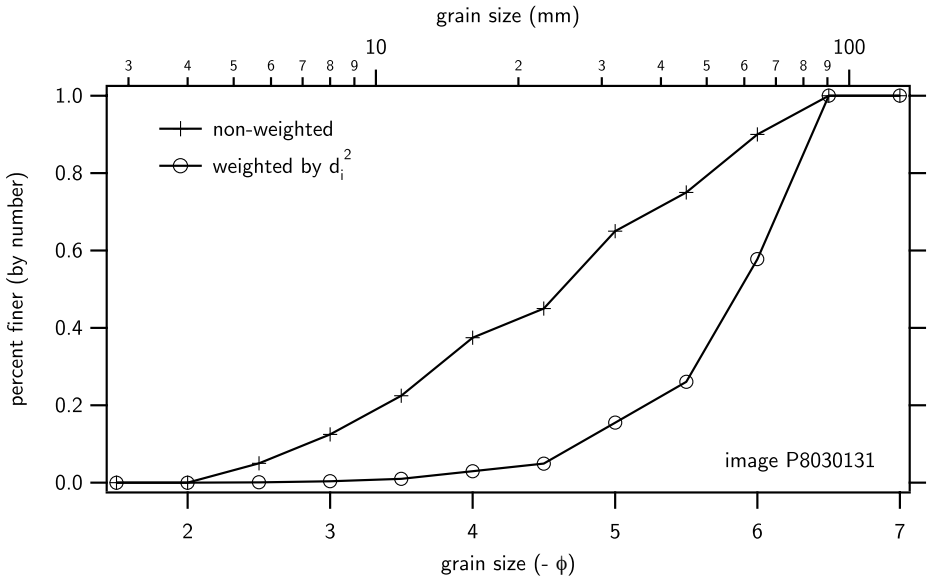

Figure 7: Site 1, image P8030131

Site 3

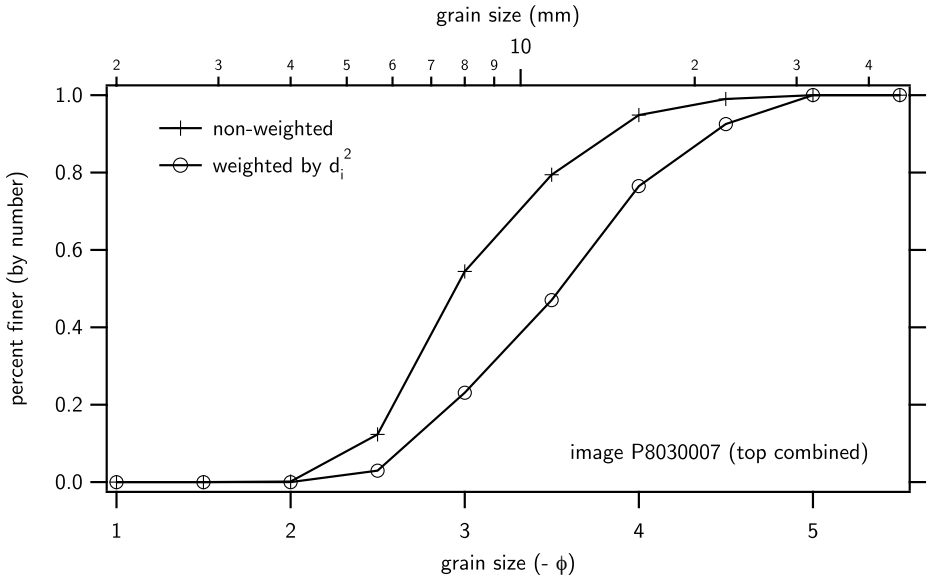

Figure 8: Site 3, image $\text{P8030007}_{top-combined}$

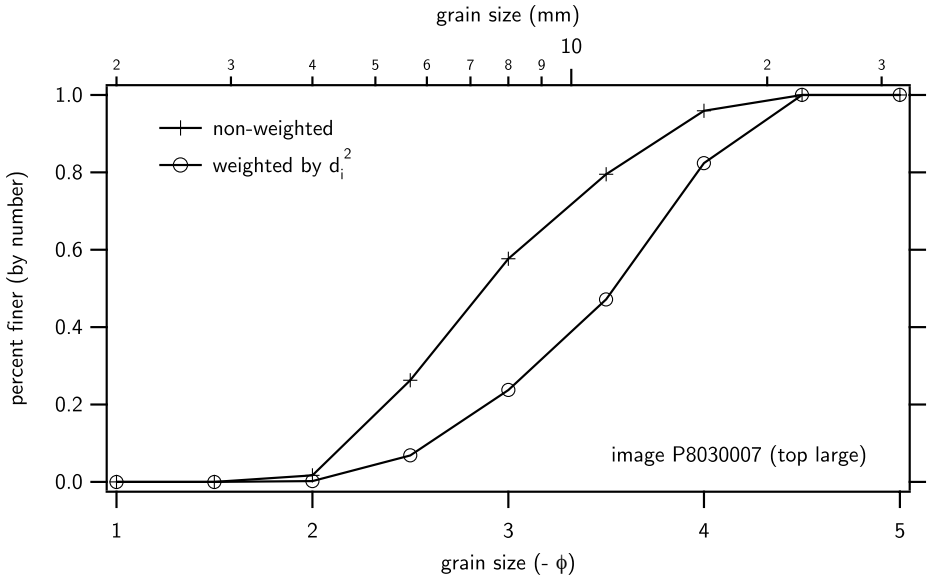

Figure 9: Site 3, image P8030007$_{top-large}$

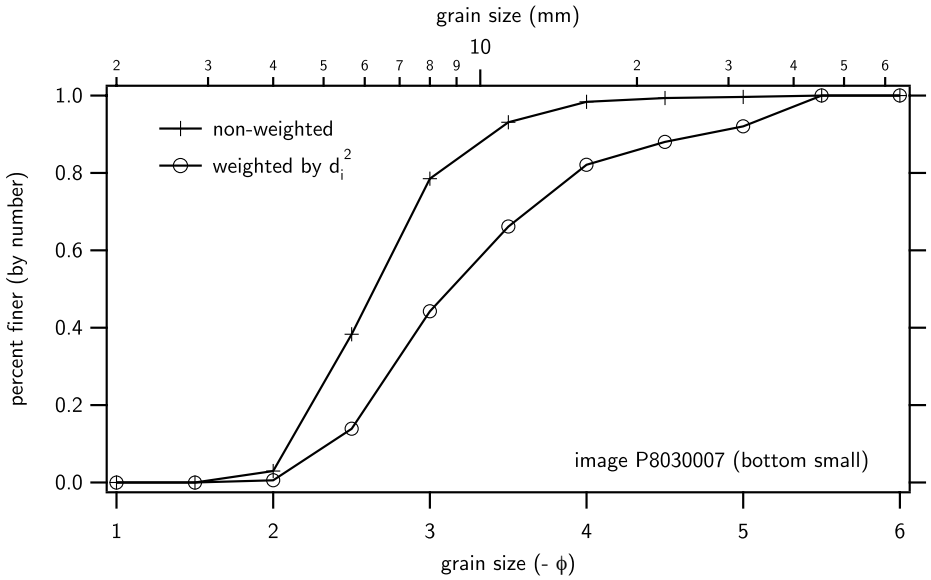

Figure 10: Site 3, image P8030007$_{bottom-small}$

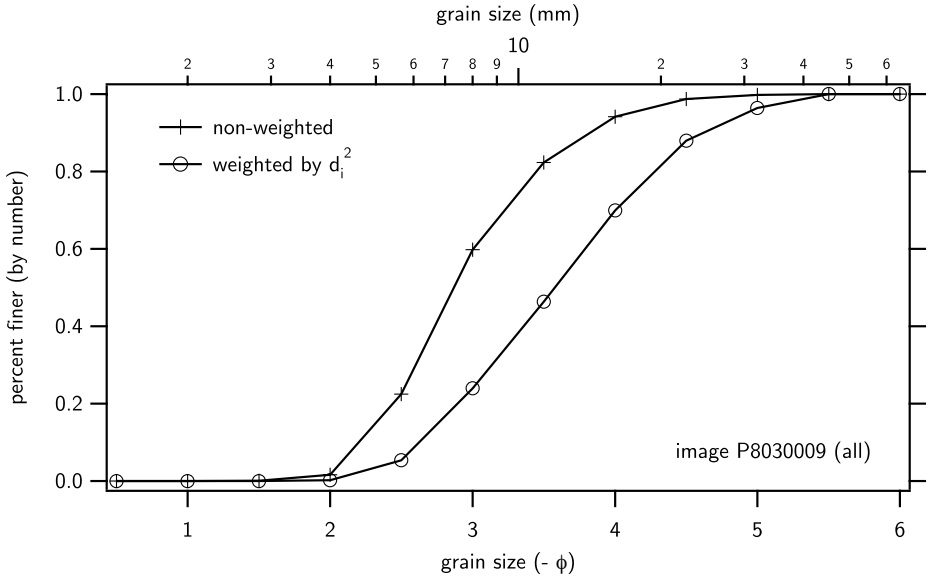

Figure 11: Site 3, image P8030009$_{all}$

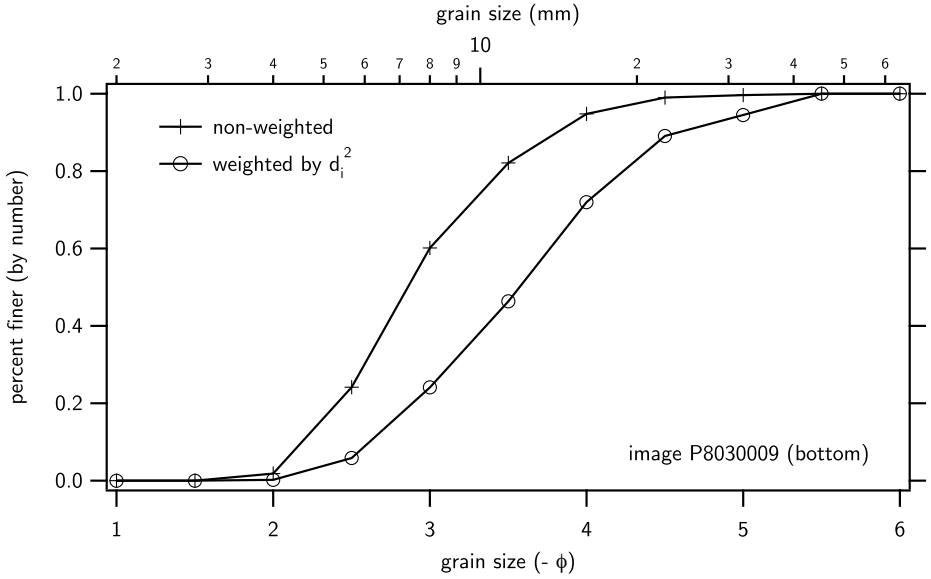

Figure 12: Site 3, image P8030009$_{bottom}$

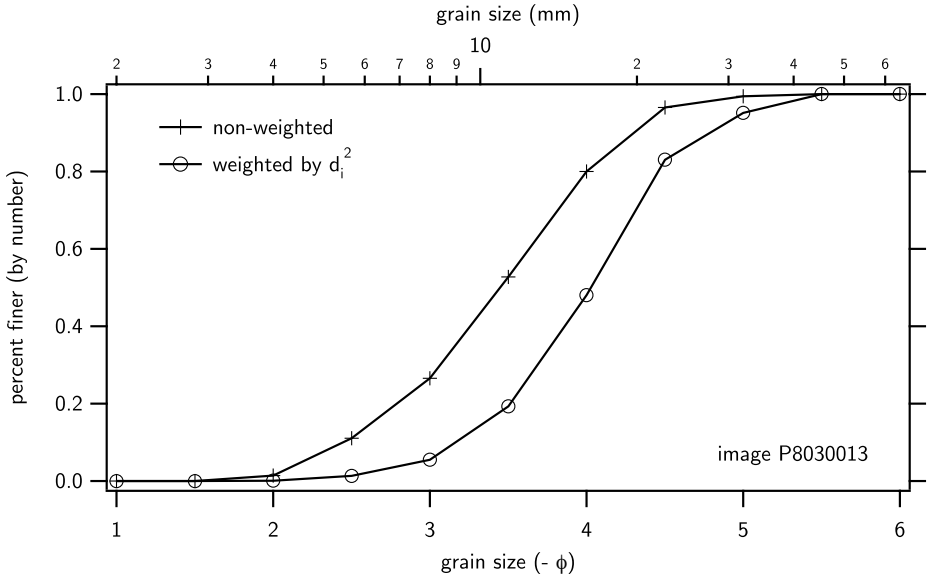

Figure 13: Site 3, image P8030013

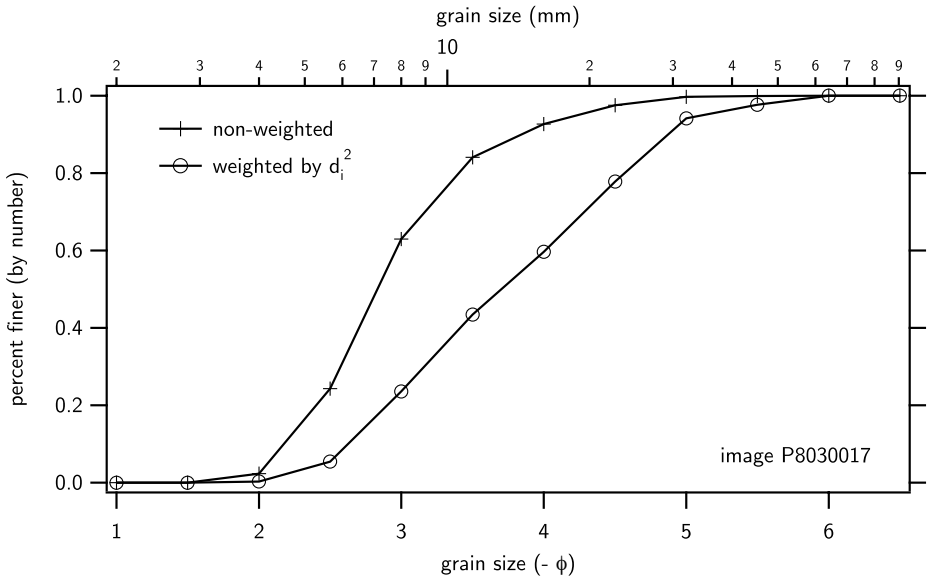

Figure 14: Site 3, image P8030017

Site 4

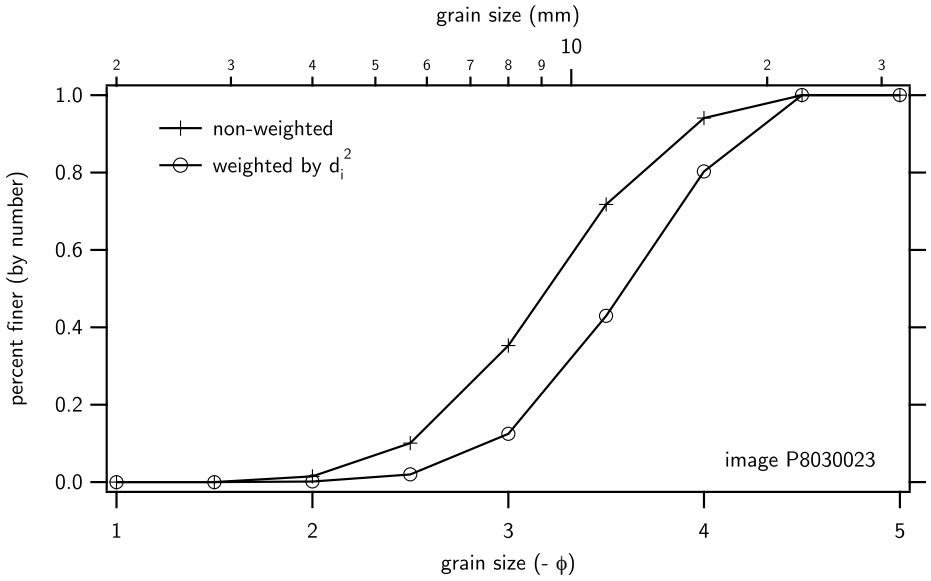

Figure 15: Site 4, image P8030023

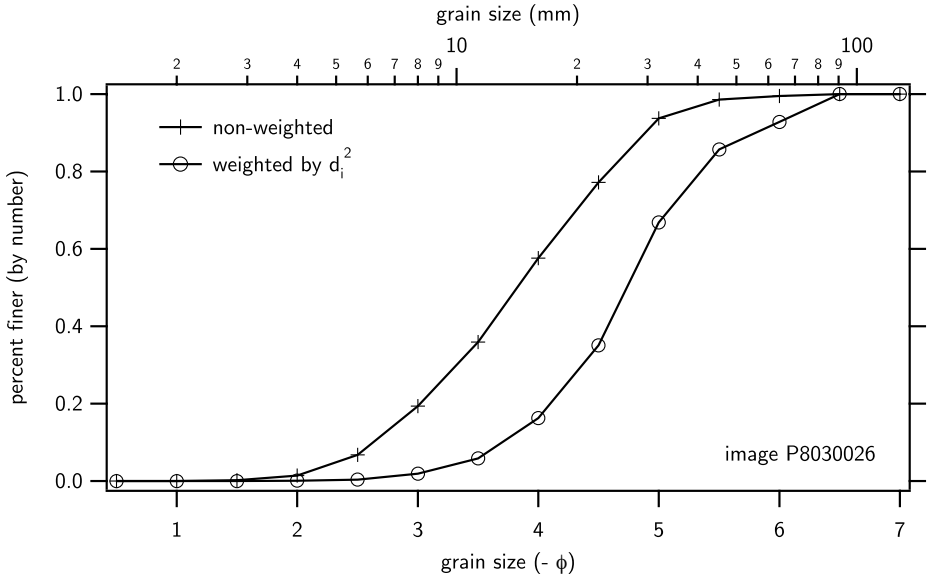

Figure 16: Site 4, image P8030026

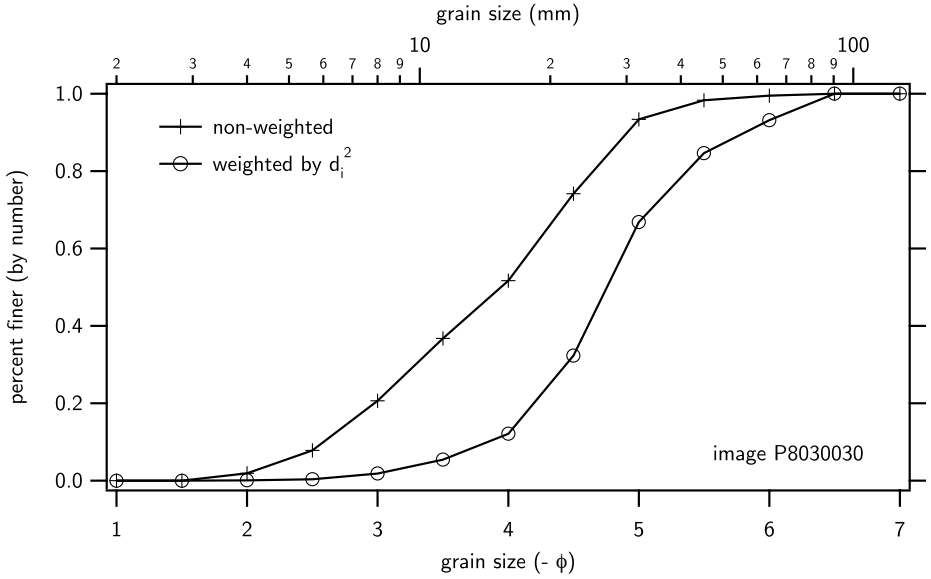

Figure 17: Site 4, image P8030030

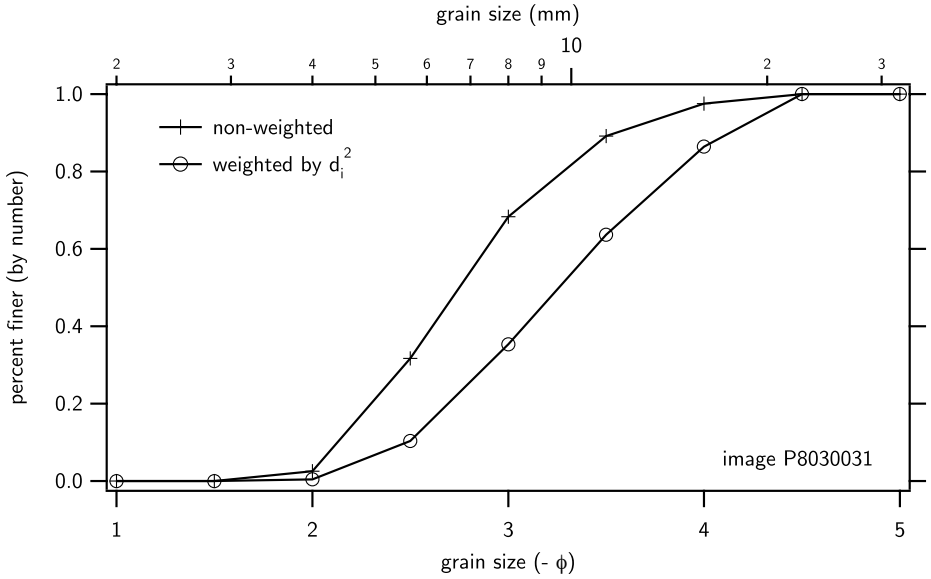

Figure 18: Site 4, image P8030031

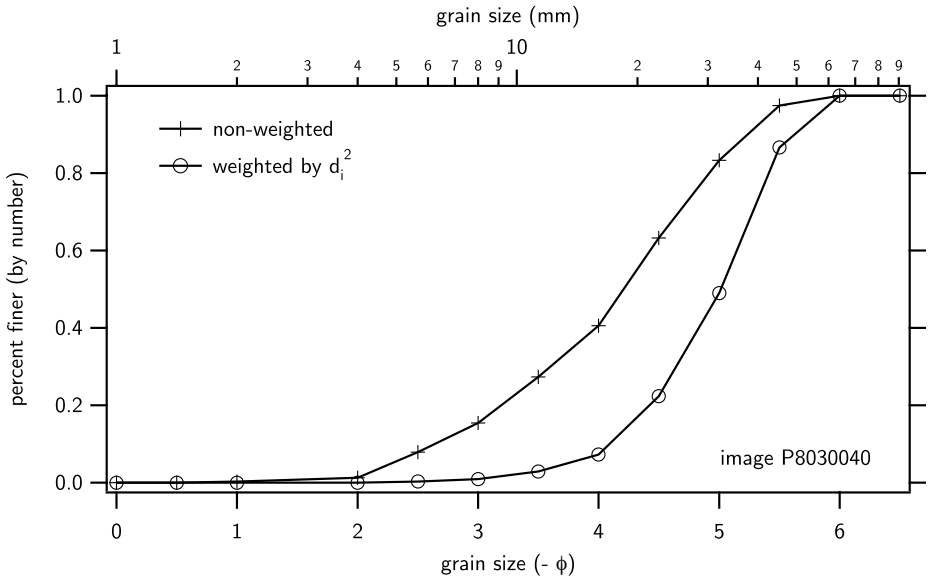

Figure 19: Site 4, image P8030040

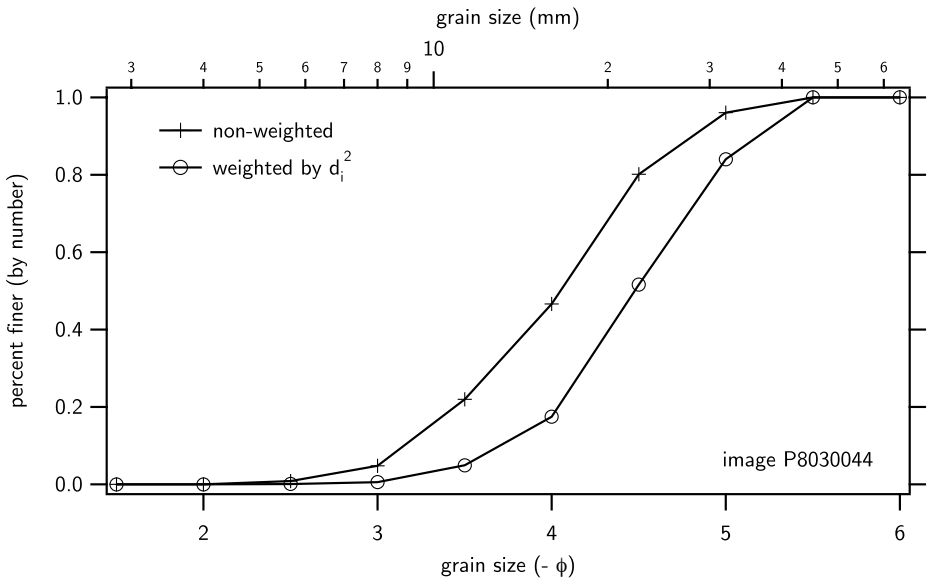

Figure 20: Site 4, image P8030044

Site 5

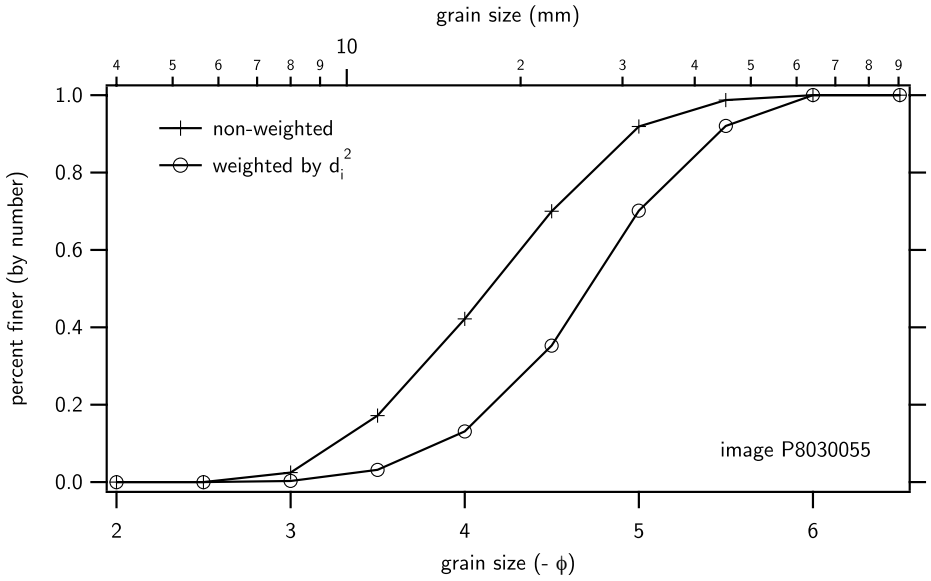

Figure 21: Site 5, image P8030055

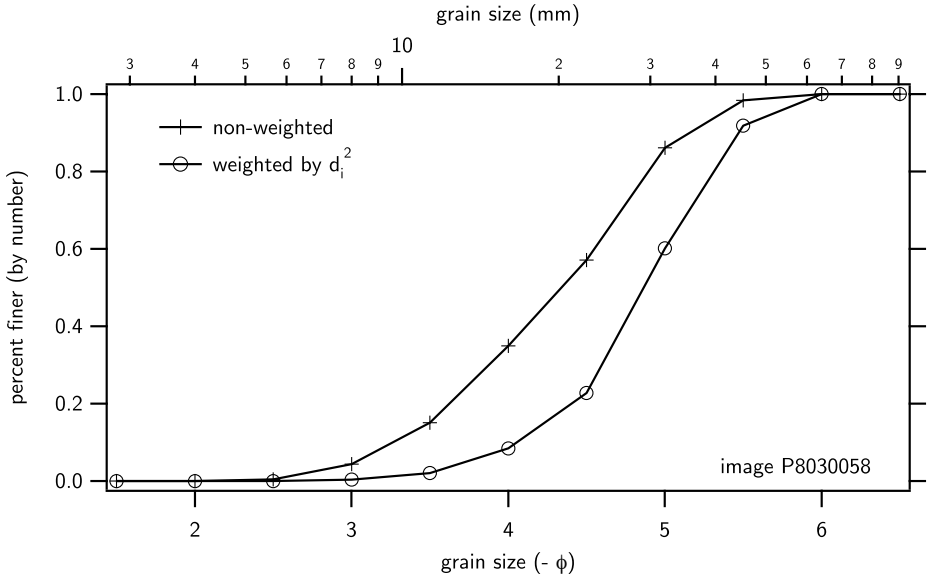

Figure 22: Site 5, image P8030058

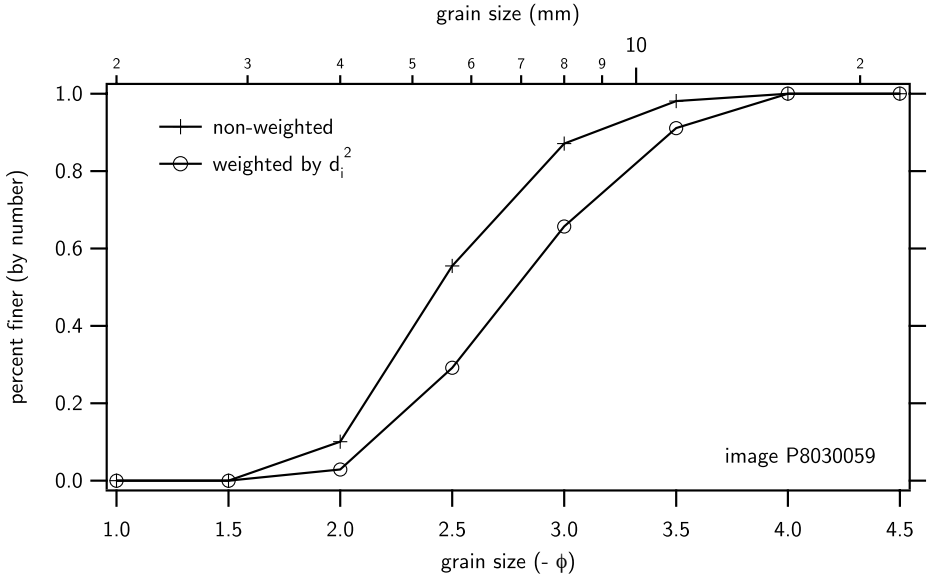

Figure 23: Site 5, image P8030059

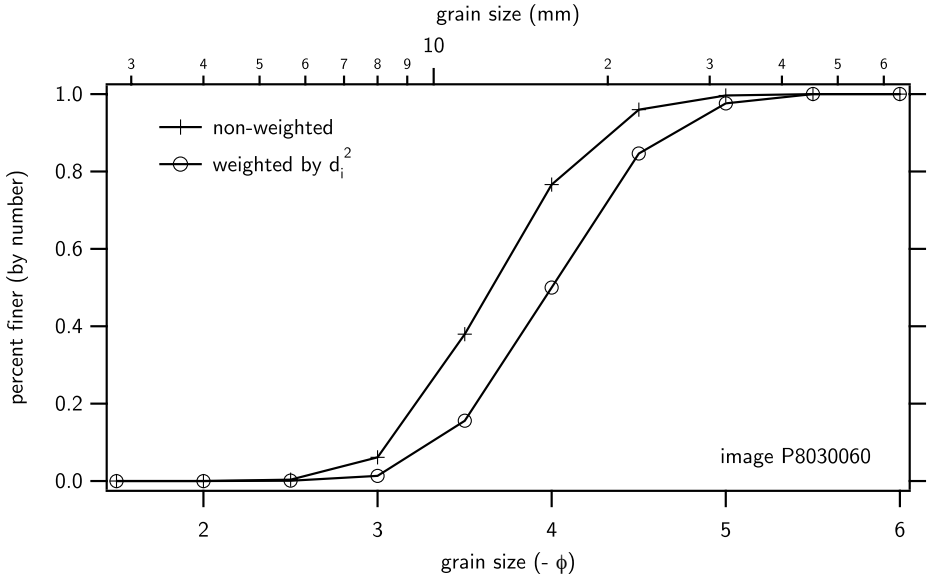

Figure 24: Site 5, image P8030060

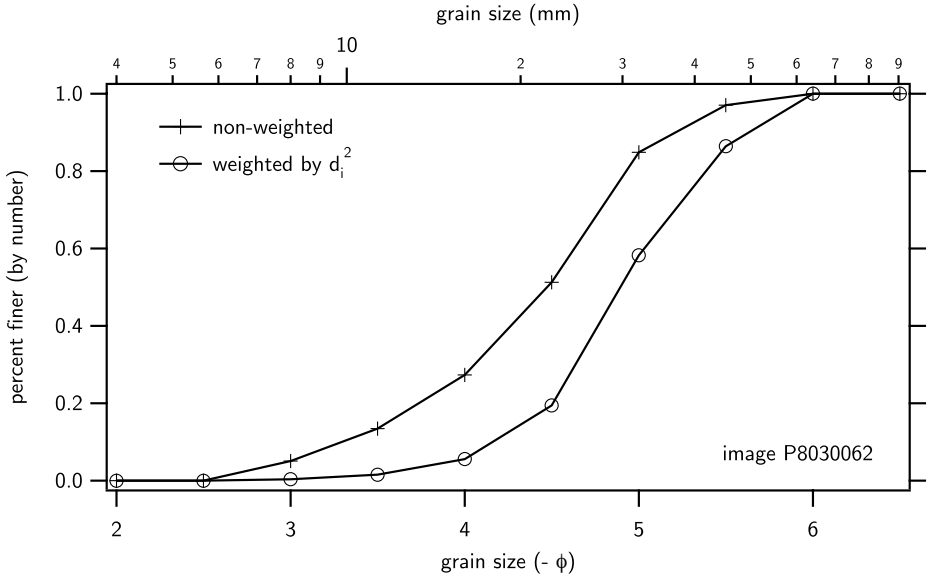

Figure 25: Site 5, image P8030062

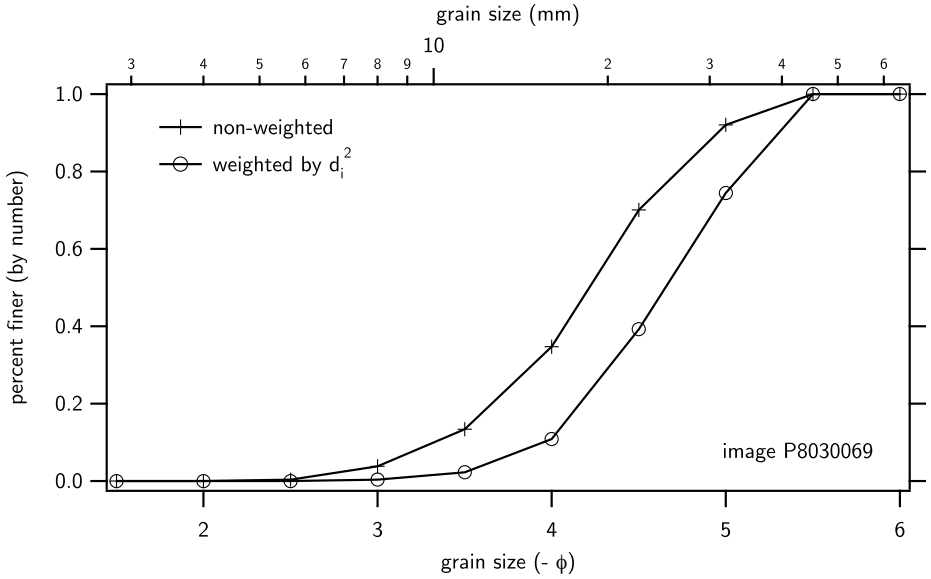

Figure 26: Site 5, image P8030069

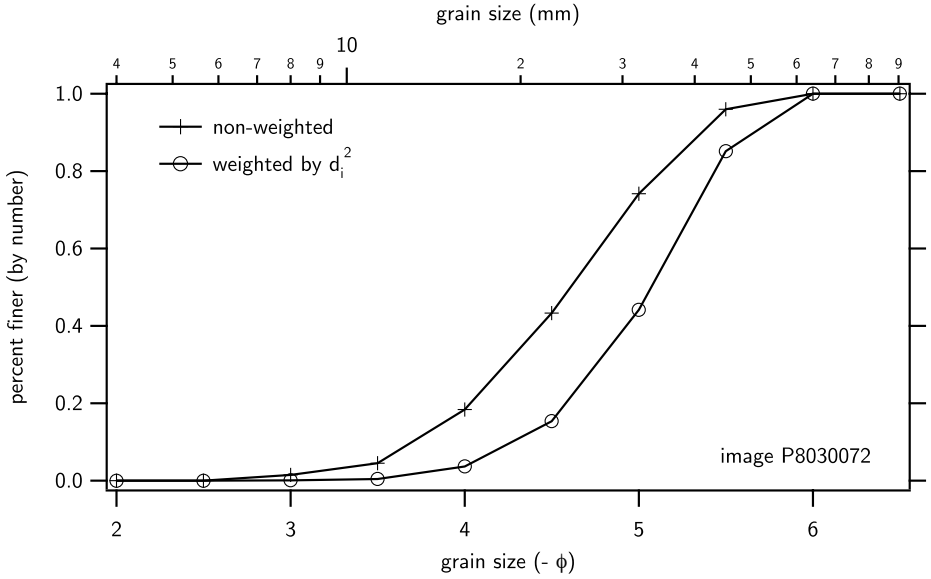

Figure 27: Site 5, image P8030072

Site 7

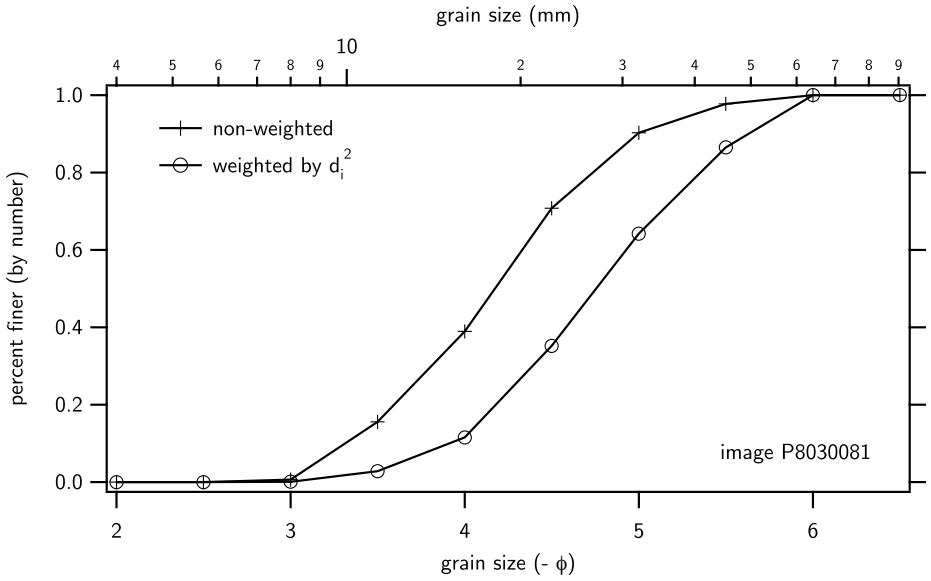

Figure 28: Site 7, image P8030081

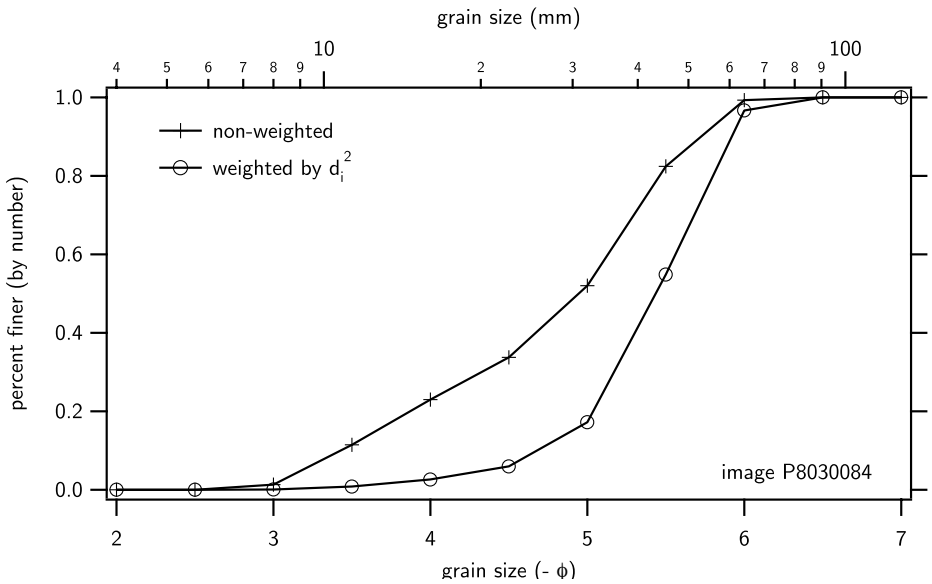

Figure 29: Site 7, image P8030084

Site 9

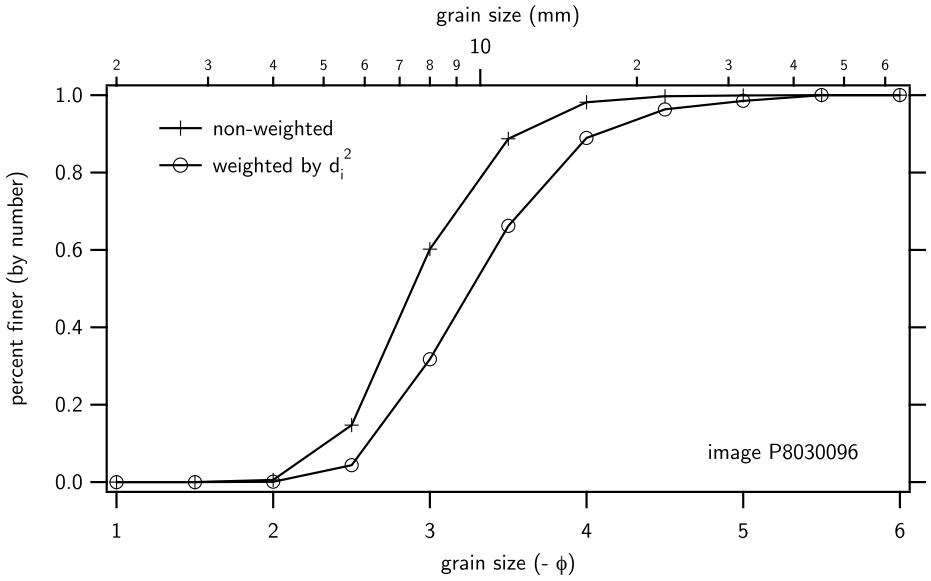

Figure 30: Site 9, image P8030096

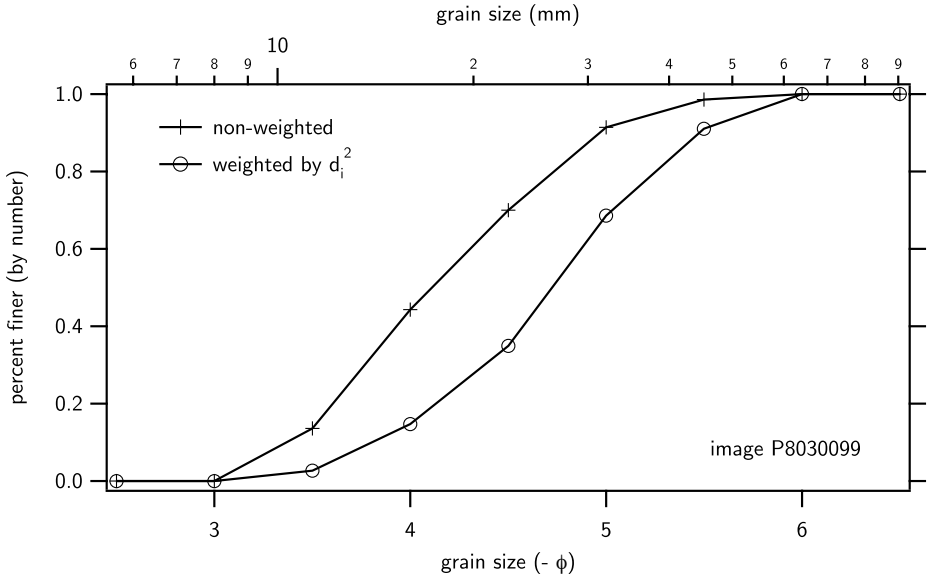

Figure 31: Site 9, image P8030099

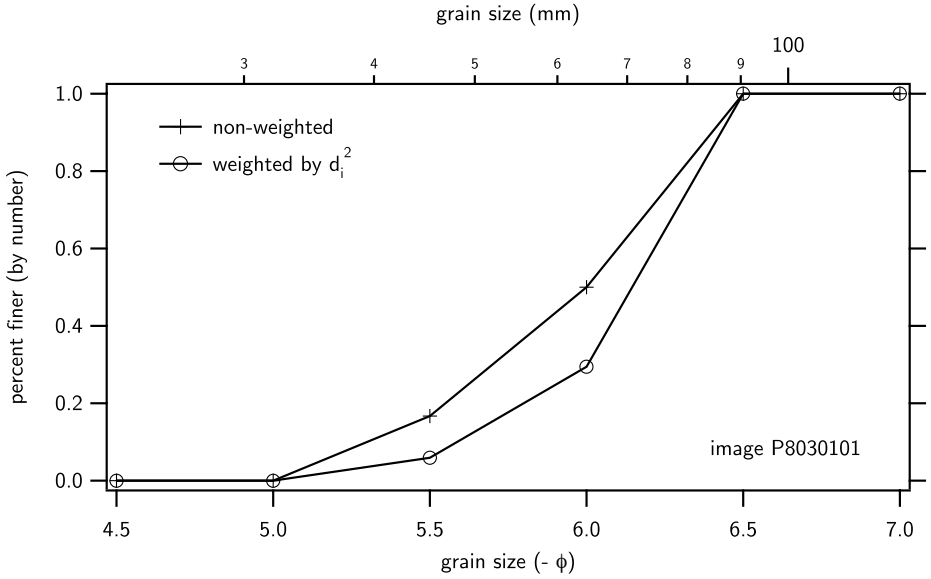

Figure 32: Site 9, image P8030101

Site 10

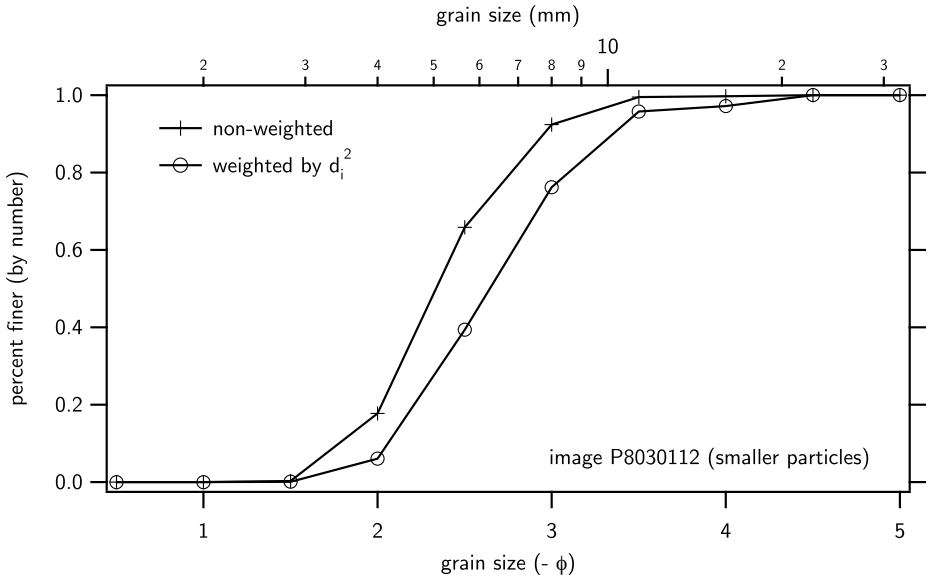

Figure 33: Site 10, image $P8030112_{smaller}$

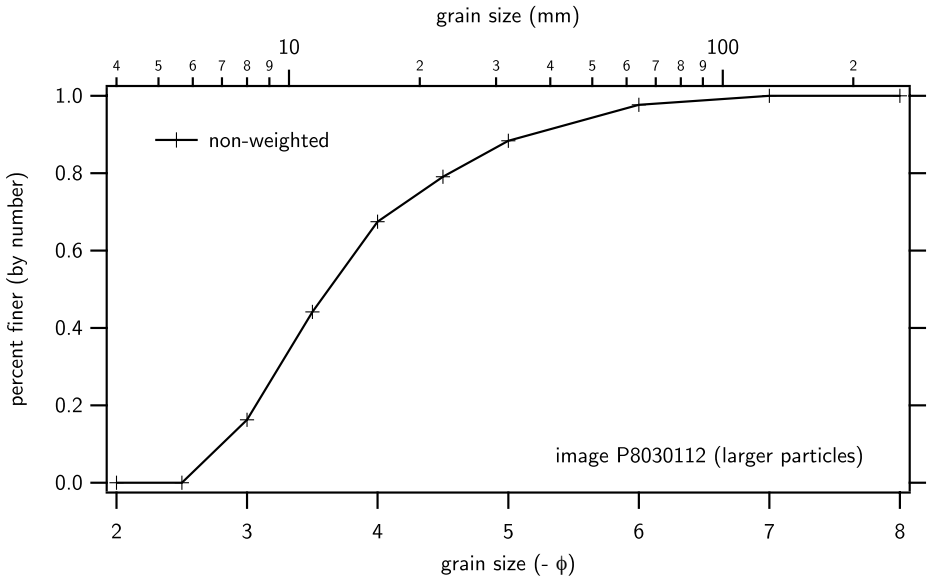

Figure 34: Site 10, image P8030112$_{larger-grid}$